






## Seasonal and habitat-based variations in vertical export of biogenic sea-ice proxies in Hudson Bay

Tiia Luostarinen <sup>1,2</sup>, Kaarina Weckström <sup>1,2,3</sup>, Jens Ehn<sup>4</sup>, Michelle Kamula<sup>4</sup>, Amanda Burson<sup>5,6</sup>, Aura Diaz <sup>4</sup>, Guillaume Massé<sup>7,8</sup>, Suzanne McGowan <sup>6,9</sup>, Zou Zou Kuzyk<sup>4</sup> & Maija Heikkilä<sup>1,2</sup>

Despite their wide use in past sea-ice reconstructions, the seasonal, habitat and species-based sources of sedimentary sea-ice proxies are poorly understood. Here, we conduct direct observations of the community composition of diatoms, dinoflagellate cysts and highly branched isoprenoid lipids within the sea ice, water column, sediment traps and sediment surface in the Belcher Islands Archipelago, Hudson Bay throughout spring 2019. We find that Arctic diatom and dinoflagellate cysts species commonly used as sea-ice proxies appear to be only indirectly linked to sea-ice conditions, and that the sediment assemblages of these groups overrepresent summertime pelagic blooms. Species contributing to the diverse sea-ice diatom communities are rare in the sediment. Dinoflagellate cysts form a typical Arctic assemblage in the sediment, although they are virtually absent in the sea ice and water column in spring. We also find that certain highly branched isoprenoid lipids that were previously considered indicators of open water, can be produced in sea-ice. We conclude that contextual knowledge and a multiproxy approach are necessary in reconstruction, encouraging further studies on the sources and controls of sea-ice proxy production in different geographic areas.

<sup>1</sup>Environmental Change Research Unit (ECRU), Ecosystems and Environment Research Programme, Faculty of Biological and Environmental Sciences, University of Helsinki, Helsinki, Finland. <sup>2</sup>Helsinki Institute of Sustainability Science (HELSUS), University of Helsinki, Helsinki, Finland. <sup>3</sup>Department of Glaciology and Climate, Geological Survey of Denmark and Greenland (GEUS), Copenhagen, Denmark. <sup>4</sup>Centre for Earth Observation Science, University of Manitoba, Winnipeg, MB, Canada. <sup>5</sup>British Antarctic Survey, Cambridge, UK. <sup>6</sup>School of Geography, University of Nottingham, Nottingham, UK. <sup>7</sup>CNRS, UMI 3376 TAKUVIK, Université Laval, Québec, QC, Canada. <sup>8</sup>UMR7159 LOCEAN, Station Marine de Concarneau, Concarneau, France. <sup>9</sup>Department of Aquatic Ecology, Netherlands Institute of Ecology (NIOO-KNAW), Wageningen, The Netherlands. ✉email: [tiia.luostarinen@helsinki.fi](mailto:tiia.luostarinen@helsinki.fi)

Sea ice is a major controller of the Earth's climate system, moderating energy balance at the planet's surface and contributing to ocean ventilation and circulation<sup>1</sup>. The ongoing rapid reductions of sea-ice area, persistence and thickness have motivated increasing efforts to resolve past sea-ice changes and their climatic causes. Multiple biogenic<sup>2</sup> and physical<sup>3–5</sup> proxies originating from the melting ice matrix preserve in underlying marine sediment archives. In particular, microscopic and biochemical fossils of ice-associated diatoms and dinoflagellates have been widely used and can provide qualitative, semi-quantitative and quantitative knowledge of past sea-ice conditions<sup>6,7</sup>. A major challenge with sea-ice reconstructions is the deficient knowledge of the habitats, environmental controls and vertical transport of many protist species and biomarkers commonly associated with sea ice.

Sea ice forms a habitat for a wide array of protists, many of which are primary producers. Both algae living within the ice (sympagic) and in the surface ocean (pelagic) need sufficient light and nutrients to thrive<sup>8</sup>. Several biogeochemically and physically distinct layers within the ice form habitats for microalgal communities<sup>9–11</sup>. Sympagic productivity is particularly high in the bottom 1–3 cm of the ice<sup>12</sup>, which is tightly coupled with the nutrient supply from the underlying seawater<sup>8</sup>. The ambient light conditions during polar spring and summer are dependent on ice and snow thickness and algal species are adapted to photosynthesis both in the ice and underneath it<sup>8,13,14</sup>. The contribution of sympagic production to the total Arctic marine primary production varies from small to notable (2–25%)<sup>8</sup>. Diatoms make up most (>90%) of the sympagic protists<sup>8</sup>, but other phylogenetic groups, such as dinoflagellates and their resting stages (cysts), are commonly observed in the ice matrix<sup>15–17</sup>. Under-ice or ice-edge blooms, following the melt onset or retreating ice-edge, are characteristic for the Arctic<sup>18,19</sup> and account for >50% of annual primary production<sup>20</sup>. Diatoms are dominant also in under-ice and ice-edge blooms, but there, dinoflagellates and other flagellates account for a larger share of the biomass compared to their minor role in the ice communities<sup>21</sup>.

Due to the pronounced seasonal light conditions in the Arctic and sub-Arctic, a pulse-like sea-ice and pelagic bloom, followed by rapid vertical transport and sedimentation, are typical across the region<sup>22–28</sup>. However, more work to improve understanding of how sediment deposits reflect contemporary water-column observations is critically needed. Microfossil species representation in the sediment archive may be affected by dissolution in the water column or at the sediment surface. It is not well known how seasonal and habitat differences and other environmental factors influencing production of protists and biomarkers used as sea-ice proxies are represented in sediment deposits. One challenge is that there are few sea-ice or water-column observations of dinoflagellate cyst species found in Arctic sediments, and their use as proxies is founded on the species distributions in surface sediments in relation to environmental conditions. Thus, many brown-coloured spiny cyst types, in particular *Islandinium minutum*, are commonly treated as sea-ice indicators based on their dominant presence in sediments from seasonally ice-covered seas<sup>29,30</sup>. In contrast, there are many field observations of sympagic and pelagic diatom species, but the laboratory methods used in standard phytoplankton studies do not allow high taxonomic resolution. While the commonly used sea-ice proxies *Fragilariopsis cylindrus*, *F. oceanica*, *F. reginae-jahniae* and *Fossilulaphycus arcticus* (e.g. <sup>31–33</sup>) are taxonomically distinct in sediment diatom preparations, there is little comparable knowledge from sea ice, water column and sinking flux. For highly branched isoprenoid lipids (HBIs), biomarkers selectively synthesised by some diatom species, there are field and laboratory studies giving insight into their sources. Notably, monoene IP<sub>25</sub> (Ice Proxy with 25 carbon atoms<sup>34</sup>) produced by

sympagic diatom species belonging to the genera *Haslea* and *Pleurosigma*<sup>35</sup> has clear sea-ice indication value. Co-occurring with IP<sub>25</sub> in the Arctic, diene IPSO<sub>25</sub> (Ice Proxy for Southern Ocean with 25 carbon atoms) synthesised at least by sympagic diatom *Berkeleya adeliensis*<sup>36</sup> is also directly sea-ice affiliated. Triene isomers HBI III and HBI IV, in their turn, are applied as indicators of pelagic production owing to their sediment distributions in ice-edge or ice-free conditions<sup>37–39</sup>. Yet, enhanced understanding of the habitat and species sources, and of the environmental controls of HBI production are required for ubiquitous application as sedimentary proxies.

In this study, we focus on the three groups of biogenic sea-ice proxies: diatoms, dinoflagellate cysts and HBIs, supported by pigment and organic geochemical data. The samples from the landfast sea ice, the under-ice water column, an automated sequencing sediment trap suspended about 40 m beneath the ice cover, and the surface sediment were collected from the Belcher Islands, south-eastern Hudson Bay (Fig. 1), over spring-summer 2019. The aim was to investigate the melt-season succession of ice-associated species and biomarkers in the ice matrix and the underlying water column, their export to the sediment and their representation in the surface of the sediment archive. Our results demonstrate previously unstudied species-specific temporal and habitat sources for diatoms, dinoflagellate cysts and HBIs, and support the notion that these sedimentary proxies are particularly valuable when used jointly. We show that sediment core diatom and dinoflagellate cyst assemblages from seasonally ice-covered environments can be dominated by species not directly affiliated with sea ice. Thus, using HBIs along with species data can improve the sea-ice reconstructions remarkably. On the other hand, species-specific assemblage data can be crucial for the interpretation of HBI data, since the known biological, seasonal and environmental controls of HBI production may not be universally applicable.

## Regional setting

The water properties in Hudson Bay are heavily influenced by Arctic Water inflow from Foxe Basin and Baffin Bay via Hudson Strait, large freshwater input from runoff (>760 km<sup>3</sup> year<sup>-1</sup>) and melting sea ice<sup>40–42</sup>. The large-scale background circulation of the Hudson Bay area follows a counter-clockwise pattern<sup>40,43</sup>, and the strong cyclonic surface current is driven by coastal freshwater inputs which causes a contrast in water masses between the coastal areas and the interior sea<sup>41,44</sup>. The Belcher Islands are located in SE Hudson Bay in Nunavut, sub-Arctic Canada (Fig. 1). The islands are rock outcrops extending over an area of 3000 km<sup>2</sup>, with a shelf area of ca. 10,000 km<sup>2</sup>, where the water depth generally varies between 0 and 40 m, but can extend to 80 m. There is a marked contrast in freshwater content in the upper water column across the Belcher Islands with the south-eastern areas of Belcher Islands strongly affected by waters with lower salinities originating mainly in James Bay (ca. 15% freshwater fraction), while the northwestern areas are more saline (ca. 5% freshwater fraction), less stratified and more representative of the interior Hudson Bay<sup>45,46</sup>. Sea ice usually forms in December, and the archipelago is fully sea-ice covered by February. Sea-ice breakup typically occurs in late June<sup>46</sup>. Coats Bay is a ca. 60 km long and 7 km wide bay in the central part of Belcher Islands that opens up towards the northwest (Fig. 1). Sea ice typically starts to form in the outer part of the bay and extends southward across the bay forming a continuous landfast ice cover, approximately 1-m thick by late winter.

## Results and discussion

**Production and vertical fluxes of biogenic proxies over spring melt.** Temperature and salinity profiles measured at the mooring

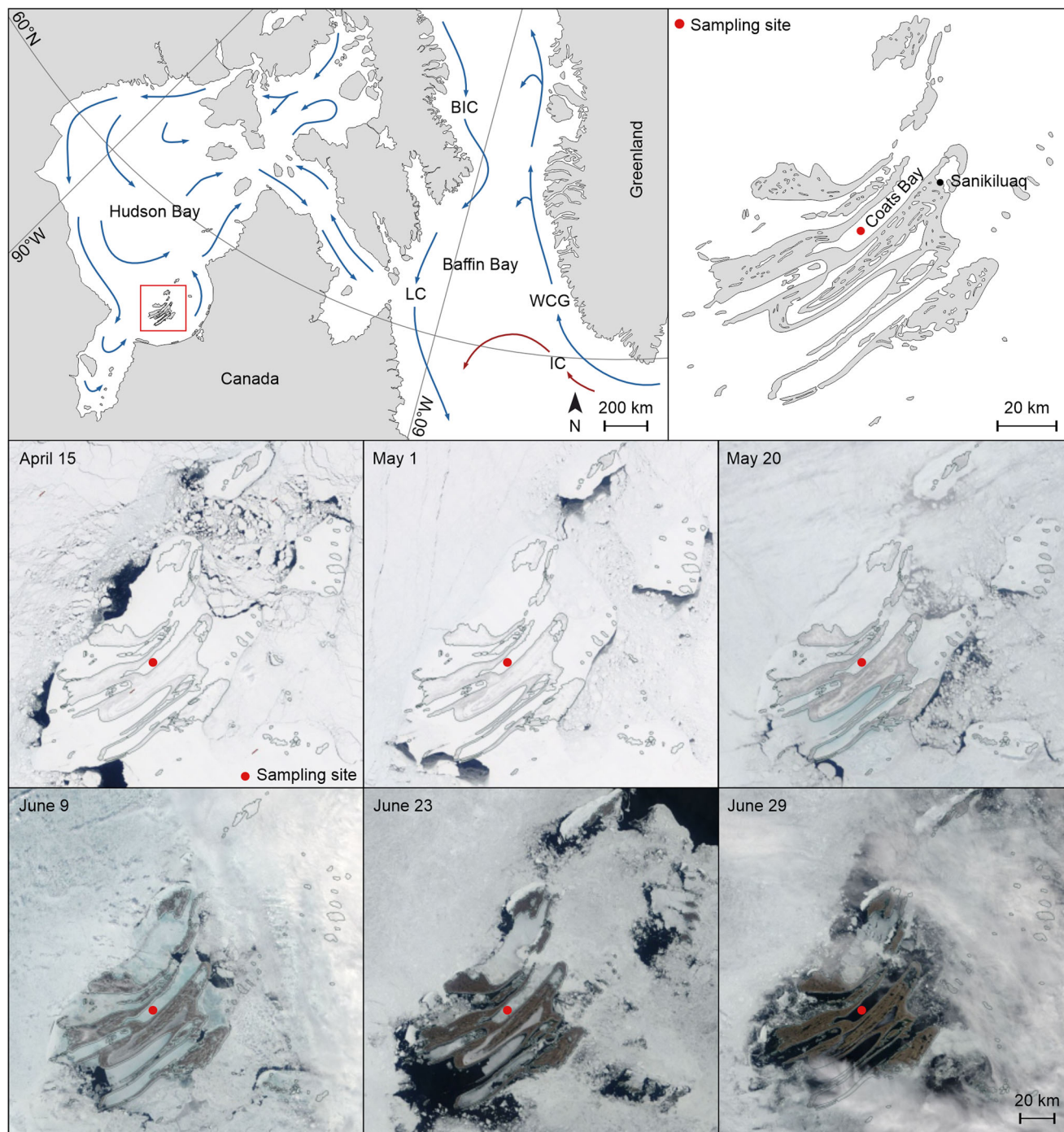


**Fig. 1 Map of the study area.** Map of the study area showing the anti-cyclonic currents in Hudson Bay as well as major cold (blue) and warm (red) currents in the area; BIC Baffin Island Current, LC Labrador Current, WGC West Greenland Current and IC Irminger Current. The sampling location is marked with a red dot. Satellite images (NASA Worldview) show the sea-ice extent over the study period.

site (Fig. 2) were representative of offshore values outside Coats Bay<sup>42,45</sup>, with relatively stable conditions followed by rapidly increasing surface water temperatures and decreasing salinities over the week of sea-ice breakup in late June (Fig. 1). Sea-ice breakup led to high fluxes of OC, diatom valves and (diatom-origin) HBIs to the sediment (Fig. 3), which is also illustrated by increasing turbidity values caused by primary production (Fig. 2).

Diatoms dominated algal communities across the sea-ice—water column—sediment continuum through the spring melt. Dinoflagellate cysts, on the other hand, were absent from sea-ice and water samples, and only two specimens, one cyst of

*Islandinium minutum* and one cyst of *Echnidinium karaense*, were recorded in the last sediment trap sample, a week after sea-ice disappearance. Calculation based on these two cysts yields an approximate dinoflagellate cyst flux of  $\sim 1000$  cysts  $m^{-2} d^{-1}$  over the week, while concomitant diatom fluxes were  $\sim 10^5$  fold higher. Algal pigment data lend support to the microscopic findings: diatom-derived fucoxanthin dominated in sea ice, while pigments indicative of dinoflagellates, such as peridinin and dinoxanthin, were absent in the samples (Fig. 3). Concentrations of fucoxanthin ( $9\text{--}100$   $nm\ l^{-1}$ ) were several times higher than Chl *a* ( $0.5\text{--}32$   $nm\ l^{-1}$ ), and the two were accompanied by other



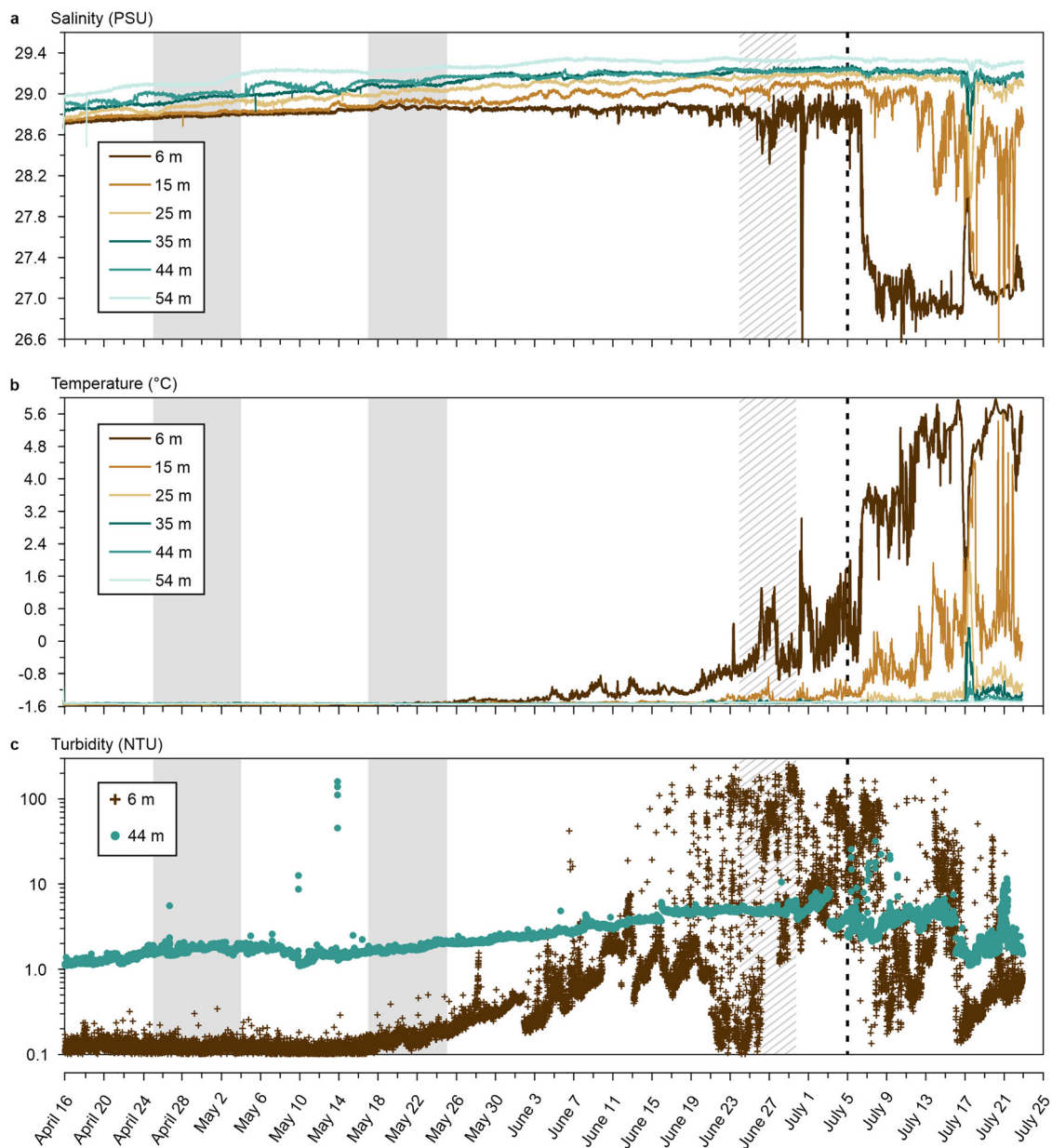


**Fig. 2** Temperature, salinity and turbidity profiles from the mooring line. **a** Salinity (PSU), **(b)** temperature ( $^{\circ}\text{C}$ ), and **(c)** turbidity profiles (NTU) measured at the mooring site at 6, 15, 25, 35, 44, and 54 metre depths. Note the logarithmic scale of the turbidity profile. The ice and water sampling periods are marked with solid grey, the end of the sediment trap sampling period with a dashed black line, and the ice breakup period with a dashed grey area.

pigments indicative of diatom production (diatoxanthin, diadinoxanthin; not plotted), and constant but minute amounts of cyanobacterial, cryptophyte and chlorophyte biomarker pigments (Fig. 3).

Sea-ice bloom at our site followed the changes in ice thickness and snowpack depth (Fig. 3). The first increase in sympagic diatom concentrations (from 4800 to 17200 valves  $\text{ml}^{-1}$ ), accompanied by heightened HBI IV, fucoxanthin and Chl *a* concentrations, was observed on April 27 when ice cover at the field site thinned from 162 cm to about 140 cm and the snowpack depth was around 15 cm (Fig. 3). The peak concentrations leveled out for the following week, with a slight increase in snowpack depth to 22–23 cm. Snowpack depth stayed at  $\sim 10$ –20 cm until mid-May, and concentrations of diatoms, algal pigments and HBIs in sea ice remained at high levels. While thick snowpack causes light limitation, moderate ( $<30$  cm) snow cover protects

ice algae, and rapid snow removal may lead to bloom inhibition<sup>47,48</sup>. At our field site, the snow layer had almost disappeared by the end of May (ca. 1–2 cm) and melt ponds started forming on the ice surface, attenuating the sympagic bloom, demonstrated by lowered diatom (5700 valves  $\text{ml}^{-1}$ ), algal pigment and HBI concentrations. Lowered under-ice salinities (Fig. 3) further indicate modifications to the bottom sea-ice habitat. Simultaneously, under-ice production and vertical export of OC and the two abundant proxies (diatoms and HBIs) to the sediment increased (Fig. 3). It is worth noting, however, that diatoms had been continuously present in minute concentrations in the water column throughout the spring.

Following the field campaign, the automated sediment trap continued weekly sampling until early July. Vertical export of OC, diatoms and biomarkers had been low through the early spring season, in particular with respect to ice-derived materials (IP<sub>25</sub>,

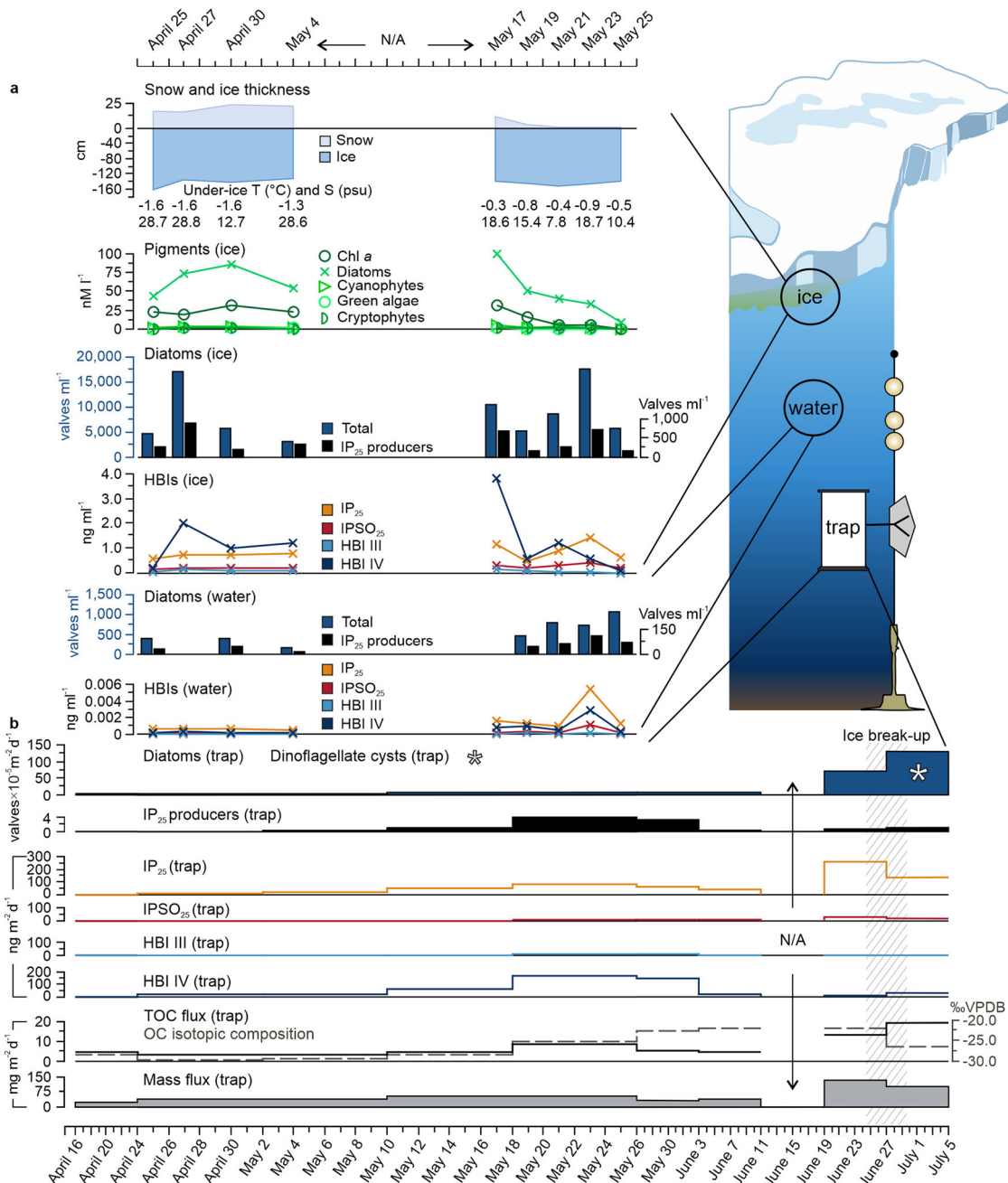


**Fig. 3 Seasonal and vertical proxy signatures in the sea ice–water column–sediment continuum.** Overall seasonal and vertical trends in proxy signatures throughout the sea-ice–water column–sediment continuum. **a** Temporal changes in snow cover and ice thickness (cm), in situ measurements of sea-surface temperature (°C) and salinity (psu), sea-ice pigment concentrations (nM l<sup>-1</sup>), total diatom concentration (valves ml<sup>-1</sup>) and IP<sub>25</sub> producing species (valves ml<sup>-1</sup>) and HBI (ng ml<sup>-1</sup>) concentrations from the sea ice and water column samples during the field campaign in April–May (upper x-axis). Pigment concentrations for diatoms = fucoxanthin, cyanobacteria = zeaxanthin and canthaxanthin, green algae = Chl b and lutein and cryptophytes = alloxanthin. **b** Total diatom flux (valves × 10<sup>-5</sup> m<sup>-2</sup> d<sup>-1</sup>), IP<sub>25</sub> producing species flux (valves × 10<sup>-5</sup> m<sup>-2</sup> d<sup>-1</sup>), HBI fluxes (ng ml<sup>-2</sup> d<sup>-1</sup>; see the exact values in Supplementary Table 3), TOC (mg m<sup>-2</sup> d<sup>-1</sup>), isotope (‰ VPDB), and mass fluxes (mg m<sup>-2</sup> d<sup>-1</sup>) from the sediment trap sampling period between April 16 to July 5 (lower x-axis). Two dinoflagellate cysts found in the last trap sample are marked with an asterisk. Note the gap in sampling period between May 4 and May 17 and a gap in the sediment trap sampling in mid-June. The sea-ice breakup period is marked with a dashed grey area.

IP<sub>SO25</sub> and respective producers; Fig. 3, Supplementary Table 3), while stable carbon isotopic (δ<sup>13</sup>C) values remained particularly low (between -29.6 and -28.5‰). Carbon dioxide supersaturation and slow algal growth in cold surface waters leads to depleted δ<sup>13</sup>C values approaching those of terrestrial OM<sup>49,50</sup>, while limited atmospheric CO<sub>2</sub> exchange underneath and within sea ice enriches the δ<sup>13</sup>C signature of ice algal and under-ice blooms (Arctic sea ice POM signatures vary between -26.4 and

-17.7<sup>51</sup>). In Hudson Bay, summer sea-surface POM values range from -23.4 to -25.9‰<sup>52</sup>. At our study site, we measured a surface sediment δ<sup>13</sup>C value of -23.3‰. In early spring, POM flux to the sediment trap had clearly more depleted δ<sup>13</sup>C, potentially due to low production in cold waters. In late May, concurrent with the snow cover disappearance and eventual sea-ice breakup, the δ<sup>13</sup>C signature rose to -25.0 to -22.0‰, signifying higher contributions from ice algal and ice-edge bloom

sources. At the same time, increasing amounts of IP<sub>25</sub> and its producers were recorded in the water column and in the sediment trap. A week after the ice breakup, the sympagic signature (fluxes of IP<sub>25</sub> and IP<sub>25</sub> producers,  $\delta^{13}\text{C}$  of OM) weakened, but export of diatoms and OC remained high.

Due to their excellent sedimentary preservation and habitat specificity in polar regions, HBIs are commonly used to reconstruct past sea-ice cover and pelagic productivity in ice-covered oceans<sup>53–58</sup>. Application of close isoprenoid analogues, mono-unsaturated IP<sub>25</sub> and di-unsaturated IPSO<sub>25</sub>, as proxies for seasonal sea ice is based on the premise of their production by few strictly sympagic diatom species and a distinct C isotopic signature<sup>34–36</sup>. In turn, the use of tri-unsaturated isomers HBI III (or HBI III Z isomer) and HBI IV (or HBI III E isomer), and more recently the ratio between the two (or HBI TR<sub>25</sub> or T<sub>25</sub><sup>59</sup>) as proxies for open-water production is founded on their pelagic diatom source<sup>60,61</sup>.

Here, the most abundant HBI in sea ice was unexpectedly HBI IV (Fig. 3). The presence of minute HBI III/IV concentrations (e.g. <sup>62,63</sup>) in sea ice could be due to under-ice phytoplankton drawn into ice. More recently, Amiraux et al. <sup>64</sup> discuss the potential sympagic origin of HBI III/IV in their data from Baffin Bay. The concentrations for HBI III/IV measured here are, however, markedly higher (peak sea-ice bloom 85–165/1200–3800 ng l<sup>-1</sup>) than those reported for HBI III/IV by Amiraux et al. <sup>65</sup> (7.4–66 ng l<sup>-1</sup>), and correspond to concentrations typical for IP<sub>25</sub> during peak sea-ice bloom. Moreover, the seasonal HBI IV trends in the ice-water-sediment continuum followed those of IP<sub>25</sub>. Both HBI IV and IP<sub>25</sub> are more abundant in sea ice (on average 1080/750 ng l<sup>-1</sup>) compared to the water column (on average 6.3/13 ng l<sup>-1</sup>). Vertical fluxes to the sediment trap over the ice-covered interval were, in their turn, dominated by HBI IV, while IP<sub>25</sub> fluxes were peaking during the ice breakup period after the main sympagic bloom. These high fluxes could possibly be explained by markedly increased IP<sub>25</sub> production induced by sympagic nutrient limitation, which has been observed towards the end of the sea ice season<sup>65</sup>: Nutrient depletion induces an increase in algal lipid synthesis and increases in HBI lipid synthesis by an order of magnitude as a result of nutrient depletion have been observed in laboratory conditions (Brown et al. <sup>66</sup> and references therein). Thus, sympagic algae may produce IP<sub>25</sub> at the end of the sea-ice season as an energy storage in preparation of unfavourable conditions during ice melt and subsequent sinking. The two other quantified HBIs, IPSO<sub>25</sub> and HBI III, were present in small amounts in all samples.

Isoprenoid IP<sub>25</sub> is a simple, excellent indicator of seasonal sea-ice conditions when found in marine sediment records, but its absence has a binary interpretation: either complete absence of sea-ice cover or perennial sea-ice cover. Thus, IP<sub>25</sub> records are often combined with a phytoplankton biomarker to form various sea-ice indices, e.g. with brassicasterol to calculate the P<sub>B</sub>IP<sub>25</sub> index<sup>67,68</sup> or with HBI III to calculate the P<sub>III</sub>IP<sub>25</sub> index<sup>37,38</sup>. These indices are used semi-quantitatively to infer sea-ice conditions directly or via a calibration set, similarly as TR<sub>25</sub> and T<sub>25</sub> indices based on HBI III/IV are used to calculate spring productivity<sup>38,58</sup>. The premise in the use of HBIs as proxies is founded on their source specificity, and uncertainty in habitat source may distort interpretations. Our results highlight the importance of further studies on HBI source species and their habitats. Since diatom species composition varies regionally, species assemblage data can have important ramifications for studies using HBIs, in particular when calculating indices such as PIP<sub>25</sub> or HBI T<sub>25</sub> in new areas.

The surface sediment sample (top 0.5 cm) incorporates sediment flux over ca. three years<sup>69</sup>. Surface sediment diatom (150,000 valves g<sup>-1</sup>) and HBI (IP<sub>25</sub> 209 ng g<sup>-1</sup>, IPSO<sub>25</sub> 23 ng g<sup>-1</sup>,

HBI III 1.8 ng g<sup>-1</sup> and HBI IV 16.4 ng g<sup>-1</sup>) concentrations were comparable to those found in pan-arctic surface sediments, and the species and isoprenoid composition resembled the sediment trap data. However, while HBI IV was the most common HBI lipid in ice and water samples, both IP<sub>25</sub> and IPSO<sub>25</sub> had higher concentrations in the surface sediment. While production of sea-ice proxy lipids IP<sub>25</sub> and IPSO<sub>25</sub> could be a late season stress response as explained above, better preservation of HBI structures with fewer double bonds could also play a role<sup>39</sup>. However, the surface sediment diatom assemblages show a much higher proportion of pelagic summer-blooming species and a markedly lower proportion of HBI-producing taxa, compared to the trap assemblages. Surface sediment dinoflagellate cyst concentration (36 000 cysts g<sup>-1</sup>) was also comparable to that of pan-arctic and Hudson Bay surface sediments, and the species composition closely matched with that reported from eastern Hudson Bay<sup>69</sup> (Fig. 5, Supplementary Table 2). Our results indicate that while diatoms dominate the sea-ice and ice-edge environments in the spring, cyst-producing dinoflagellates bloom later in the summer and autumn.

We highlight that specific proxy types and indices are not universally applicable, and underline the need for contextual knowledge in both qualitative and quantitative sea-ice reconstruction. In the coastal system studied here, diatoms almost exclusively dominate the spring season sympagic and pelagic communities based on both microscopic and biomarker data, and they constitute the bulk of vertical export of biogenic matter, while dinoflagellates and their cysts are nothing short of absent from all spring season samples despite forming a typical Arctic assemblage in the surface sediment. This implies that dinoflagellate cyst species may not have a direct sea-ice indication value, and their use as sea-ice proxies requires careful, site-specific consideration and more experimental evidence.

**Diatom community dynamics and HBI producers.** The sea-ice samples collected during April and May 2019 reveal a diverse community that includes a marked number of species, which are not found in the sediment trap or in the surface sediment, while sharing many species with the water-column diatom community (Figs. 4–6, Supplementary Table 1). The sea-ice samples included a total of 121 diatom taxa compared to a total of 72 taxa in the water-column samples taken during the same period (Supplementary Table 1). The most common genera and the most abundant species within each genus in the ice and the underlying water-column (0–30 m) were pennate taxa such as *Nitzschia* (*N. frigida*, *N. neofrigida*, *N. hudsonii*), *Navicula* (*N. directa*, *N. septentrionalis*, *N. transitans* incl. sub-species, *N. valida*), *Pleurosigma* (*P. stuxbergii*, *P. rhomboides*), *Diploneis* (*D. littoralis* var. *clathrata* and var. *arctica*), *Pinnularia* (*P. quadratarea* incl. several varieties, *Pinnularia semiinflata*), *Pseudogomphonema* (*P. septentrionale*, *P. groenlandicum*) and *Stenoneis* (*S. inconspicua* var. *baculus*), amounting to >99% and >90% of all taxa enumerated in the sea ice and water column, respectively.

The Hudson Bay sea-ice communities share the marked contribution of *Nitzschia* and *Navicula* species with other seasonally sea-ice covered Arctic regions (e.g. <sup>26,70–74</sup>). However, they also host a relatively high abundance of *Diploneis*, *Pinnularia* and notably *Pleurosigma* species (Fig. 5, see further discussion on HBI producers), uncommon in the other studies cited. The dominance of pennate benthic species (adapted to living attached to a surface) in the sea ice and (released into) the underlying water column is likely facilitated by the long ice-cover period, which allows for this unique community to fully develop<sup>75</sup>. *Melosira arctica*, another common Arctic sub-ice diatom species, was only observed in the surface sediment as a minor component

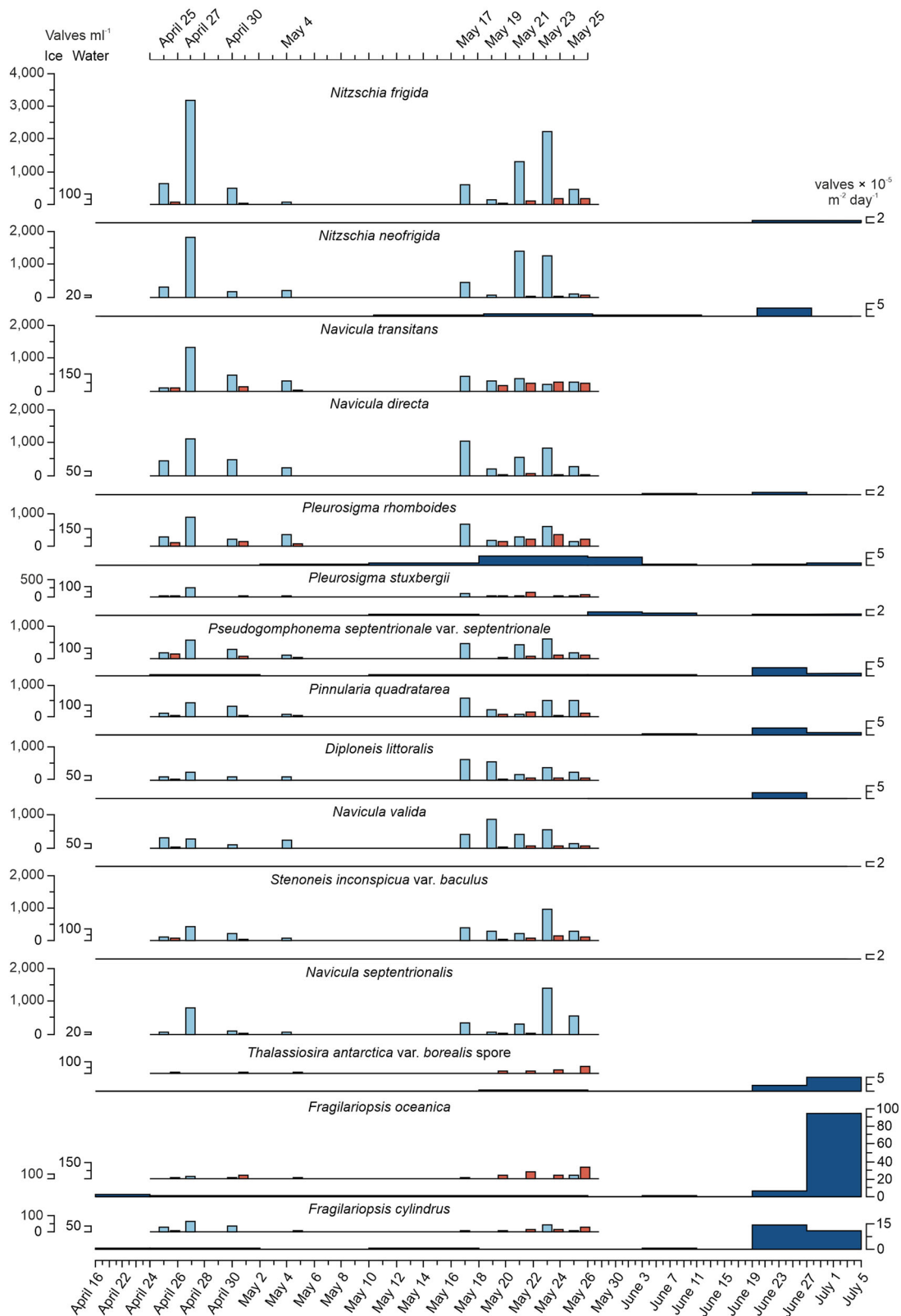


**Fig. 4** Diatom concentrations and fluxes in sea ice, water column and sediment trap samples. Diatom concentrations (valves ml<sup>-1</sup>) from sea ice (light blue) and water column (orange) samples between April 25 and May 25, and diatom fluxes (valves × 10<sup>-5</sup> m<sup>-2</sup> d<sup>-1</sup>) from the sediment trap (dark blue silhouette) between April 16 and July 5. Note that not all species are shown here but are listed in Supplementary Table 1. Note the gap in sampling period between May 4 and May 17 and a gap in the sediment trap sampling in mid-June.



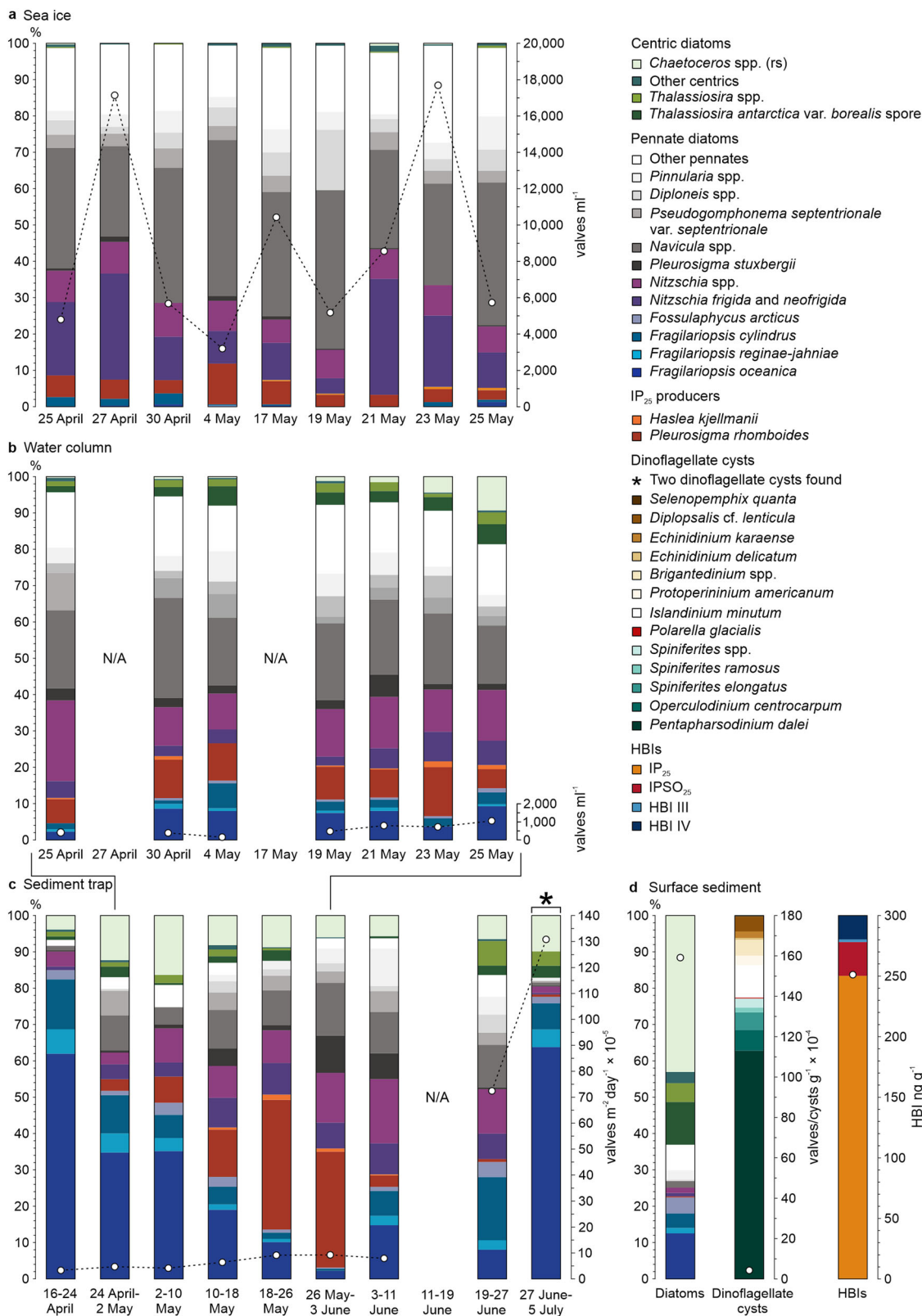


**Fig. 5** Relative abundances of the proxies in sea ice, water column, sediment trap and surface sediment samples. Relative abundances (%) of the diatom taxa in (a) sea ice, (b) water column, (c) sediment trap and (d) surface sediment samples, dinoflagellate cysts and HBIs in surface sediment. Dinoflagellate cysts present in any other than surface sediment samples are marked with an asterisk. Total diatom concentrations (valves ml<sup>-1</sup>; (a) sea ice, (b) water column, valves g<sup>-1</sup> × 10<sup>-4</sup>; (d) surface sediment), total diatom flux (valves m<sup>-2</sup> d<sup>-1</sup> × 10<sup>-5</sup>; (c) sediment trap), total dinoflagellate cyst concentration (cysts g<sup>-1</sup> × 10<sup>-4</sup>; (d) surface sediment), and total HBI concentration (ng g<sup>-1</sup>; (d) surface sediment) are marked with white circles connected with a black dashed line.



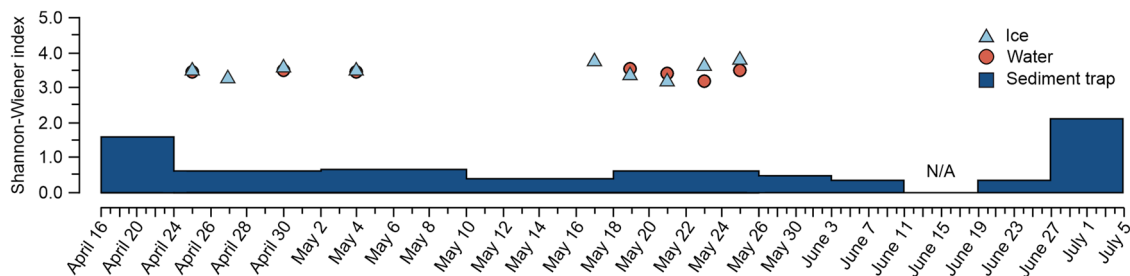


**Fig. 6** Diatom species diversity in sea ice, water column and sediment trap samples. Shannon-Wiener diversity indices for sea ice (light blue triangle), water column (orange circle) and sediment trap (dark blue silhouette) samples during the sampling periods.

of the assemblage (<2%), presumably as it has a strong association to multi-year ice<sup>72</sup>.

The water column communities showed a clearly larger portion of the sea-ice associated spring blooming species *Fragilariopsis oceanica*, *F. cylindrus*, *F. reginae-jahniae* and *Fossilaphycus arcticus*, which inhabit the marginal ice zone (Weckström et al.<sup>33</sup> and references therein). Centric *Thalassiosira* taxa were present at moderate abundances (up to ca. 10%), most notably *T. antarctica* var. *borealis* resting spore (listed as *T. gravida* spore in many earlier studies), which is associated with less-stratified open-water environments (compared to the MIZ<sup>31,57</sup>).

The sediment trap samples contained a notably lower number of taxa compared to the sea ice and water column (58 in total excluding *Chaetoceros* resting spores; Fig. 6). While the dominant species and genera were mostly shared with the sea ice and water column, the three *Fragilariopsis* species and *Fossilaphycus arcticus* were clearly more abundant than in these above-lying habitats in particular after the ice breakup. Of these four species, *F. oceanica* is by far the most abundant. Also, the centric pelagic *Thalassiosira* taxa were markedly more abundant and diverse in the trap samples, which, unlike the sea-ice and water-column samples, extend to late July (Fig. 5). Further, while many of the less abundant species found in sea ice and underlying water column were not present in the sediment trap, it also hosted species not found in these above-lying habitats (Supplementary Table 1).

The surface sediment sample, encompassing the diatom production of one to several years, reveals an assemblage more similar to the trap samples than the sea ice or water-column samples. However, there are also marked differences: species forming the marginal ice zone/early pelagic spring bloom (*Fragilariopsis* species, *Fossilaphycus arcticus*; >20%), *Thalassiosira* species and other centric taxa (such as *Bacterosira bathyomphala*, *Sinerima marigela*, *Melosira arctica*, *Porosira glacialis*) comprise ca. 75% of the assemblage (Fig. 5), while the abundance of pennate taxa typical to the other habitats (*P. rhomboides*, *Nitzschia*, *Navicula*, *Pinnularia* and *Pseudogomphonema* species) is much lower, suggesting the surface sediment assemblage is dominated by spring and summer open-water production.

The species diversity, assessed using the Shannon-Wiener diversity index, was notably higher in the sea ice and in the water-column compared to the sediment trap and surface sediment, as expected based on species numbers in each habitat (Fig. 6). The sea-ice assemblages had the highest diversity, aligning with findings elsewhere in the Arctic<sup>17,72</sup>. Based on these results, it appears that many of the rarer and/or lightly silicified species found in the sea ice and the water column either do not make it to the seafloor (dissolution, predation), or are diluted by the more abundant pelagic spring blooming species.

The sea-ice communities in Hudson Bay appear to be more diverse compared to several other detailed studies on sympagic

communities in seasonal sea-ice environments (based on species numbers<sup>57,75,76</sup>). Their diversity is, however, clearly lower compared to the exceptionally high species number reported from Chukchi Sea first-year ice<sup>71</sup>. It is also important to note that diatom species diversity in multi-year ice is on average higher than in first-year ice<sup>76</sup>, which covers Hudson Bay in the winter.

The sea ice and water column proportional species compositions (Fig. 5) are similar to each other throughout the sampling season (April–May). There is minor temporal variability, the most notable changes observed in the ice between the relative abundance of *Nitzschia frigida* + *N. neofrigida* and *Navicula* species, with the former dominating especially in late April (when snow and sea ice thickness were momentarily reduced) and in mid-May. The minor seasonal variability in Hudson Bay sea-ice community composition differs markedly from a similar study in NE Greenland, where sea-ice community composition was highly variable over the spring season<sup>26</sup>. In NE Greenland, the sympagic diatom spring bloom started during the one-month study period and was brief, similarly to the pelagic diatom bloom in this High-Arctic setting. In the more southern Hudson Bay, the sympagic spring bloom appears to have begun already before the start of the study period, which could partly explain the lower seasonal variability observed here.

In contrast, the sediment trap data displays marked variability in the proportional species composition of diatom assemblages throughout the sampling season (April–July) (Figs. 4, 5). Overall, the *Fragilariopsis* species and *Fossilaphycus arcticus* dominate from mid-April to early May and again towards the end of June (up to ca. 85% of the total assemblage). Their dominance in mid-April to early May is likely due to advection of these species to the still ice-covered study site from nearby partially open-water areas (MIZ environments, see satellite images in Fig. 1). This is supported by the generally low diatom concentration (white circles in Fig. 5). From mid-May to early June, the trap assemblages have a closer resemblance to the sea-ice species composition and are dominated by *Pleurosigma rhomboides* (up to ca. 40%), indicating a release of diatoms from the sea-ice matrix at our study site.

The individual diatom species concentrations in ice and water (Fig. 4) largely follow the trends in total diatom concentrations throughout the study period (Fig. 3): Most sea-ice diatoms are found only at low concentrations in the water column and in the sediment trap, while some species, such as *Navicula septentrionalis*, are completely absent. An exception to this observation is the species *Pleurosigma rhomboides*, which dominates the trap samples in May and early June when the ice starts melting (Figs. 4, 5). Taxa that have been traditionally considered sea-ice species especially in paleoceanographic studies (*Fragilariopsis* taxa<sup>32</sup>) and the *Thalassiosira antarctica* var. *borealis* spore are found in the sea ice and in the underlying water column at notably low concentrations, but these species dominate the trap samples in late June and early July around the transition from ice

cover to open-water (Figs. 1, 4). Underrepresentation of the sea-ice taxa in sediment trap and surface sediment has also been observed in other studies. While diatom composition from traps under multi-year ice resembles sea-ice communities, diatom assemblages from traps under seasonal sea ice are dominated by the pelagic spring bloom. The markedly higher biomass of the pelagic spring bloom compared to the ice algal bloom is reflected in the vertical diatom export, and hence dominates the diatom species assemblage found in the traps/sediment<sup>72,76</sup>. In addition, the preservation of the often lightly silicified sea-ice taxa may play a role (Limoges et al.<sup>26</sup> and references therein).

Of the known IP<sub>SO<sub>25</sub></sub> and IP<sub>25</sub> producers<sup>6,35</sup>, we found *Pleurosigma rhomboides* and *Haslea kjellmanii*. The latter was detected only in the sea ice at relative abundances <0.7%, whereas *Pleurosigma rhomboides* was present at moderate to high relative abundances in all habitats (Fig. 5), apart from the surface sediment, where it was rare (1% of the total assemblage). This may be due to the aforementioned open-water spring bloom diluting the sympagic signal in the surface sediment sample, which presents an order of magnitude longer period of formation compared to the other samples (sea ice, water column, sediment trap). Its abundance in the sea ice samples was markedly higher than the combined abundance of the known IP<sub>25</sub> producers found in Arctic sea ice at a number of locations<sup>35</sup>. All four HBIs were detected in the surface sediment, suggesting that the lipid biomarkers may better indicate the presence of sea ice in instances where the diatom species producing these lipids are found in small numbers or their siliceous valves have not been preserved.

Both HBI III and HBI IV were present in the sea-ice samples, with HBI IV as the most abundant HBI type, which contrasts with many previous studies, and may change the interpretation of these biomarkers as sea-ice related proxies (see discussion in section “Production and vertical fluxes of biogenic proxies over spring melt” and references therein). However, as none of the known HBI III or HBI IV producing species (*Pleurosigma intermedium*, certain *Rhizosolenia* species and *Berkeleya rutilans*<sup>60</sup>) were found in any of our samples, it could be possible that these HBIs are also produced by other (yet unknown) sea-ice diatom species. As seen in Figs. 3, 4, *Pleurosigma rhomboides* and HBI concentrations are near coeval throughout the spring succession. Hence, another and more likely explanation may be that *Pleurosigma rhomboides* produces all four types of HBIs in the sea ice, which are then released into and/or possibly produced in the water column. This remains to be verified by future studies on *P. rhomboides* cultures.

## Conclusions

Diatoms, dinoflagellate cysts and HBI lipids produced by certain sympagic and pelagic diatom species are valuable paleoclimatological proxies in sea-ice covered environments. The interpretation of these proxies with respect to sea-ice conditions is however not universal. Instead, their sea-ice signatures are affected by factors such as nutrient availability, salinity and light regime, and importantly, as our study from southeastern Hudson Bay further indicates, by the temporal bloom windows and biogeography of the species.

Diatoms dominated the sea-ice blooms in our data and the sympagic diatom community was diverse compared to that of the sinking flux, and especially the surface sediment. Dominant sympagic diatom species, including HBI synthesiser *Pleurosigma rhomboides*, were also common in the spring sinking flux. The contribution of sympagic species to the surface sediment assemblage was however insubstantial, likely due to the dilutive effect of high biomass contribution from pelagic blooms later in the season. The typical sea-ice proxy species *Fragilariopsis oceanica*, *F.*

*cylindrus*, *F. reginae-jahniae* and *Fossilulaphycus arcticus* encompassed limited concentrations in sea ice and water-column samples, but dominated the sinking flux after the ice breakup, and made up >20% of the surface sediment diatom assemblage. Dinoflagellate cysts, in their turn, were strikingly near absent in the ice, water column and sediment trap samples. The surface sediment dinoflagellate cyst assemblage, however, composed of typical concentrations of Arctic species. Thus, notably, the sediment dinoflagellate cyst assemblage is likely represented by late season bloomers solely. Our seasonal study highlights the understudied and multifaceted associations of diatom and dinoflagellate cyst species with the sea-ice environment and points out that the common sedimentary sea-ice proxy species are in fact not directly affiliated with sea ice. Thus, contextual understanding is critical for their use in qualitative and quantitative sea-ice reconstruction. Enhanced understanding of the seasonal sources, environmental preferences and behaviour of these species (and assemblages) across the ice-water-sediment continuum will crucially benefit interpretation of sediment core data.

Analysis of HBIs from the sediment can offer valuable insights into past sea-ice conditions, and notably complements interpretations based on species assemblage data, and vice versa. However, we highlight the importance of improving the understanding of the effects of growth conditions (nutrients, salinity and light), and of HBI source species and habitats. To date, HBI IV has been considered an open-water indicator. Based on our results, it appears that HBI IV can also be produced in the sea-ice matrix, likely by *P. rhomboides*. We underline that the interpretation of HBI records found in Arctic sediments could also be dependent on the regionally dominant sea-ice diatom species producing these lipids. Furthermore, in our data, the dominance of sea-ice proxy IP<sub>25</sub> in the late season HBI flux and in the surface sediment contrasts the fact that it was not a governing contributor to the total HBI concentration during the peak sympagic bloom. We thus highlight the need for studies of HBI production over the final sea-ice disappearance.

## Methods

**Sample collection.** A 66 m mooring line was deployed on 12 April 2019 in Coats Bay (56.256°N; 79.422°W). The set-up included an upward-looking RDI WorkHorse Acoustic Doppler Current Profiler (ADCP) at 65-m depth, seven RBR solo CT sensors at different depths (6 m, 15 m, 25 m, 35 m, 44 m, 53.5 m, and 65 m), two turbidity sensors at 6-m and 44-m depths, and an automated Gurney Instruments Baker-style, cylindrical sediment trap (aperture 0.032 m<sup>2</sup>) at 40-m depth, 30-m above the seafloor. The sediment trap collected material at 8-day intervals over 80 days from mid-April to late-June 2019 (Table 1). Prior to deployment, the collector cups were filled with formalin and sodium borate with a salinity adjusted to 40 per mil. The samples were stored in a cold room at 4 °C until further processing. Zooplankton swimmers were removed by sieving the samples through a 180-µm stainless steel sieve. The samples were wet-split into eight subsamples using a HAVER RPT Rotating Sample Reducer at Aarhus University, Denmark.

The surface sediment (top 0.5 cm) sample was collected using a Kajak-Brinkhurst gravity corer, designed to preserve the soft water-sediment surface interface, and deployed through a hole in the ice at the site of trap deployment on April 15, 2019 (the day before sediment trap sampling began). The sediment samples were stored at +4 °C until further processing.

Sea ice, seawater and plankton net samples were collected at 2- to 5-day intervals during the field campaign from late April to late May 2019, with a gap between the sampling dates in early May (Table 1). The sampling site (56.33°N; 79.40°W) was located close to the sediment trap deployment, but far enough away to allow undisturbed sedimentation. Each sampling day, snow and ice cover depths (average of ten measurements), under-ice seawater temperatures and salinities (CTD cast with RBR Concerto® and CastAway-CTD® sensors) were measured, and ten sea-ice cores, a seawater sample (0–30 m) and a plankton net sample were collected (Table 1). Sea-ice cores were extracted with a Kovacs Mark II core barrel with an internal diameter of 9 cm (Kovacs Ent., Lebanon, U.S.A.). The bottom-most 5 cm of each ice core was sealed into a sampling bag, transported and stored frozen in the dark until further treatment. The samples were melted at the field camp within 12 h from sampling. To prevent the algae from going into hypo-osmotic shock<sup>77</sup>, the ice samples were melted with filtered (0.2 µm polycarbonate filters) sea water collected in situ, using a 1:3 ice:water volumetric ratio. After melting, the ice sample representing ten core bottoms was carefully mixed. For

**Table 1 The sediment trap, water column and ice core sampling dates and intervals.**

Trap interval Start date	Trap interval End date	Trap interval # of days	Ice/water sampling date
16.4.2019	24.4.2019	8	
24.4.2019	2.5.2019	8	25.4.2019
			27.4.2019
			30.4.2019
2.5.2019	10.5.2019	8	4.5.2019
10.5.2019	18.5.2019	8	17.5.2019
18.5.2019	26.5.2019	8	19.5.2019
			21.5.2019
			23.5.2019
			25.5.2019
26.5.2019	3.6.2019	8	
3.6.2019	11.6.2019	8	
11.6.2019	19.6.2019	8	
19.6.2019	27.6.2019	8	
27.6.2019	5.7.2019	8	

diatom and dinoflagellate cyst analyses, 500-ml subsamples were stored in amber glass bottles (+4 °C), fixed with 1% acidic Lugol's solution to prevent microbial growth. For HBI and algal pigment analyses, 1000 ml of the ice sample (for each analysis) was filtered onto Whatman GF/F (0.7 µm pore size) glass fibre filters and stored frozen.

Water samples (17.5 L) were collected with a 2.5 L Kemmerer water sampler by pooling seawater from 2.5-, 5-, 10-, 15-, 20-, 25- and 30-metre depths. The sample was well mixed and two 500 ml subsamples for microscopic analyses were fixed with 1% Lugol's solution and stored in amber glass bottles (+4 °C). For HBI and pigment analyses, 3000 ml of the water sample (for each analysis) was filtered onto Whatman GF/F (0.7 µm pore size) glass fibre filters and frozen until further treatment.

The plankton net (Ø 18 cm, 10 µm) haul covered the top 30 m of the water column. The net was rinsed into a 250 ml amber glass bottle and fixed with 1% acidic Lugol's solution. The samples were stored in +4 °C. The plankton net samples were used for diatom and dinoflagellate cyst analyses.

**Mass fluxes, TOC fluxes and δ<sup>13</sup>C.** For sediment total organic carbon (TOC) and δ<sup>13</sup>C analyses, inorganic carbon was removed with hydrochloric acid (HCl) fumigation (sediment trap samples) or rinse (surface sediment sample) methods<sup>78</sup>. The sediment trap samples were filtered onto pre-combusted Whatman GF/F filters, fumigated with 12 M HCl in a desiccator for 12 h, and dried at 60 °C. The surface sediment sample was treated with 10% liquid HCl for 24 h, rinsed with distilled water until neutral and freeze-dried. All samples were packed in silver capsules prior to analysis by Elementar Vario EL Cube elemental analyser (Elementar Analysensysteme GmbH, Hanau, Germany) interfaced to an Isoprime VisION IRMS (Elementar UK Ltd, Cheadle, UK) at the UC Davis Stable Isotope Facility, USA.

**Diatom and dinoflagellate cyst analysis.** Diatom slides from sea ice, seawater, sediment trap and surface sediment samples were prepared using standard paleolimnological methods<sup>79</sup> at the Marine Biology Laboratory, University of Helsinki. Prior to preparation, the samples were left to settle in an Utermöhl chamber for 24 h, after which the settled material was rinsed into a glass beaker, treated with 30% hydrogen peroxide for 4 h to remove organic material and with 10% hydrochloric acid to remove inorganic carbon. The samples were subsequently rinsed multiple times with deionized water. After the last rinse, 1 to 15 drops of microscope solution with a concentration of 6.03 × 10<sup>5</sup> spheres per ml was added into each sample. One to two drops of the sample were left to dry on cover slips and mounted onto permanent glass slides with Naphrax<sup>™</sup>.

Dinoflagellate cyst slides from the sea ice, water and sediment trap samples were prepared at the Marine Biology Laboratory, University of Helsinki, after first settling samples in an Utermöhl chamber for 24 h. The settled material was rinsed into a glass beaker and *Lycopodium clavatum* marker grains<sup>80–82</sup> were added to each sample in order to estimate cyst concentrations and fluxes. Samples were treated with 10% hydrochloric acid to remove inorganic carbon and subsequently rinsed with deionized water. Dinoflagellate cyst slides were mounted with glycerine jelly, using ~1 ml of prepared suspension per slide. The dinoflagellate cyst slide from the surface sediment sample was prepared using standard palynological methods at the laboratory of Research Unit Palaeontology, Ghent University, Belgium. *Lycopodium clavatum* marker grains were added to the sample, which was subsequently treated with 6% HCl and 40% HF to digest carbonates and silicates, respectively. The remaining organic fraction was then sieved with a 20-µm nylon mesh. About a millilitre of material remaining on the mesh was mounted on a microscope slide with glycerine jelly.

Diatom species were identified according to Poulin and Cardinal<sup>83–85</sup>, Cremer et al.<sup>86</sup> and Witkowski et al.<sup>87</sup>, with a Zeiss Axio Imager.A2 upright research microscope, Plan-Apochromat 100×/1.4 oil immersion objective, phase contrast optics and a total magnification of ×1000. At least 300 diatom valves (600 for the surface sediment sample) were identified to species level whenever possible. Co-occurring *Chaetoceros* spp. resting spores were enumerated. Dinoflagellate cyst species were identified according to Radi et al.<sup>88</sup> and Zonneveld and Pospelova<sup>89</sup> using Plan-Apochromat 60×/1.4 oil immersion objective, bright-field optics, and a total magnification of ×600. At least 300 dinoflagellate cysts (surface sediment), or a minimum of 500 *Lycopodium clavatum* marker grains (sea ice, water, sediment trap), were counted.

**Biomarkers and pigments.** The filters from ice and water samples, as well as sediment from trap and core top samples, were freeze-dried and sent to the TAKUVIK research laboratory at the University of Laval, Canada, for HBI analysis. The extraction, identification and quantification followed the protocols described by Belt et al.<sup>34,60,90</sup>. Prior to lipid extraction an internal standard (7-hexylnonadecane and 9-octylheptadecene) was added to each filter and freeze-dried sediment sample to allow quantification. The samples were saponified in a methanolic KOH solution (ca. 4 ml H<sub>2</sub>O:MeOH 1:8; 5% KOH) for 2 h at 90 °C. Hexane (3 × 1 mL) was added to the saponified content, with non-saponifiable lipids transferred to clean vials and dried over N<sub>2</sub> (30 °C). The non-saponifiable lipids were then re-suspended in hexane (0.5 mL) and fractionated using open column chromatography (SiO<sub>2</sub>; 0.5 g) prior to analysis by gas chromatography mass spectrometry (GC-MS). Procedural blanks and standard sediments were run every 15 samples. Hydrocarbon fractions were analysed using an Agilent 7890 GC (30 m) 50 m fused silica columns; 0.25 mm internal diameter and 0.25 µm film thickness) coupled to an Agilent 5975 C series mass selective detector (MSD). Oven temperatures were programmed as follows: 40–300 °C at 10 °C min<sup>-1</sup>, followed by an isothermal interval (at 300 °C for 10 min). Data were collected and analysed with Agilent Chemstation software. HBIs were identified by comparison of retention indices and mass spectra to those of authentic standards.

The filters for ice chlorophyll and carotenoid pigments were kept frozen and sent for analysis at the University of Nottingham, UK. Freeze-dried sediment was extracted in a mixture of acetone/methanol/water in a ratio of 80:15:5 in a freezer at -4 °C for 24 h. Extracts were then filtered with a 0.22-µm-pore PTFE filter, dried under N<sub>2</sub> gas, re-dissolved in an acetone/ion-pairing reagent/methanol mixture with a ratio of 70: 25: 5, and then injected into an Agilent 1200 series high-performance liquid chromatography unit. Pigments were separated using a modification of Chen et al.<sup>91</sup> and identified and quantified based on their retention time and absorption spectra, compared with pigment standards<sup>92</sup>. To calculate pigment concentrations, chromatogram peak areas were calibrated using commercial standards (DHI Denmark). Linear regressions (r > 0.99) of mass pigment injected (as volume × concentration) and peak area were used for calibration<sup>93</sup>.

## Data availability

The datasets generated during and/or analysed during the current study are archived in the PANGAEA data repository at <https://doi.org/10.1594/PANGAEA.955160>. The satellite imagery is provided by NASA's Worldview application, part of NASA's Earth Observing System Data and Information System (EOSDIS), freely available at <https://worldview.earthdata.nasa.gov>.

Received: 3 June 2022; Accepted: 15 February 2023;

Published online: 16 March 2023

## References

- Dieckmann, G. S. & Hellmer, H. H. The importance of sea ice: an overview. In: *Sea Ice, 2nd edition*, (Eds. Thomas, D. & Dieckmann S.) 1–22 (Blackwell Publishing Ltd, 2009).
- de Vernal, A., Gersonde, R., Goosse, H., Seidenkrantz, M.-S. & Wolff, E. W. Sea ice in the paleoclimate system: the challenge of reconstructing sea ice from proxies—an introduction. *Quat. Sci. Rev.* **79**, 1–8 (2013).
- Andrews, J. T. et al. A robust, multisite Holocene history of drift ice off northern Iceland: implications for North Atlantic climate. *Holocene* **19**, 71–77 (2009).
- Lisitzin, A. P. Stages of lithogenesis in ice zones – three types of sea ice sedimentation and two vertical levels of the process. In: *Sea-ice and Iceberg Sedimentation in the Ocean, Recent and Past* (Eds. Lisitzin, A.P.) 79–115 (Springer, Berlin, 2002).
- Darby, D. A. Sources of sediment found in sea ice from the western Arctic Ocean, new insights into processes of entrainment and drift patterns. *J. Geophys. Res. Oceans* **108**, 3257 (2003).
- Belt, S. T. Source-specific biomarkers as proxies for Arctic and Antarctic sea ice. *Org. Geochem.* **125**, 277–298 (2018).



7. Heikkilä, M., Ribeiro, S., Weckström, K. & Pienkowski, A. J. Predicting the future of coastal marine ecosystems in the rapidly changing Arctic: The potential of palaeoenvironmental records. *Anthropocene* **37**, 100319 (2022).
8. Arrigo, K. R. Sea ice as a habitat for primary producers. In: *Sea Ice, 3rd Edition* (Ed. Thomas, D.N.) 352–369 (Wiley-Blackwell, 2017).
9. Horner, R. et al. Ecology of sea ice biota. I. Habitat, terminology, and methodology. *Polar Biol.* **12**, 417–427 (1992).
10. Arrigo, K. R. Sea Ice Ecosystems. *Ann. Rev. Mar. Sci.* **6**, 439–467 (2014).
11. Petrich, C. & Eicken, H. Overview of sea ice growth and properties. In: *Sea Ice 3rd Edition* (Ed. Thomas, D.N.) 1–41 (Wiley-Blackwell, 2017).
12. Brown, T. A. et al. Temporal and vertical variations of lipid biomarkers during a bottom ice diatom bloom in the Canadian Beaufort Sea: further evidence for the use of the IP25 biomarker as a proxy for spring Arctic sea ice. *Polar Biol.* **34**, 1857–1868 (2011).
13. Palmisano, A. C., Beeler SooHoo, J. & Sullivan, C. W. Effects of four environmental variables on photosynthesis-irradiance relationships in Antarctic sea-ice microalgae. *Mar. Biol.* **94**, 299–306 (1987).
14. van Leeuwe, M. et al. Microalgal community structure and primary production in Arctic and Antarctic sea ice: A synthesis. *Element. Sci. Anthropocene* **6**, 4 (2018).
15. Montresor, M., Lovejoy, C., Orsini, L., Procaccini, G. & Roy, S. Bipolar distribution of the cyst-forming dinoflagellate *Polarella glacialis*. *Polar Biol.* **26**, 186–194 (2003).
16. Gast, R. J. et al. Abundance of novel dinoflagellate phylotype in Ross Sea, Antarctica. *J. Phycol.* **42**, 233–422 (2006).
17. Niemi, A., Michel, C., Hille, K. & Poulin, M. Protist assemblages in winter sea ice: setting the stage for the spring ice algal bloom. *Polar Biol.* **34**, 1803–1817 (2011).
18. Perrette, M., Quartly, G. D., Popova, E. E. & Yool, A. Pan-Arctic view of ice-edge phytoplankton blooms. In: *Proceedings of ESA Living Planet Symposium*, Bergen, Norway, 28th June–2nd July 2010, ESA, SP-686 (2010).
19. Arrigo, K. R. et al. Massive Phytoplankton Blooms Under Arctic Sea Ice. *Science* **336**, 1408 (2012).
20. Sakshaug, E. Primary and Secondary Production in the Arctic Seas. In: *The Organic Carbon Cycle in the Arctic Ocean* (Eds. Stein, R. & McDonald, R.W.) 57–81 (Springer, 2004).
21. Poulin, M. et al. The pan-Arctic biodiversity of marine pelagic and sea-ice unicellular eukaryotes: a first-attempt assessment. *Mar. Biodivers.* **41**, 13–28 (2011).
22. Bauerfeind, E., Garrity, C., Krumbholz, M., Ramseier, R. O. & Voß, M. Seasonal variability of sediment trap collections in the Northeast Water Polynya. Part 2. Biochemical and microscopic composition of sedimenting matter. *J. Mar. Syst.* **10**, 371–389 (1997).
23. Rysgaard, S., Nielsen, T. G. & Hansen, B. Seasonal variation in nutrients, pelagic primary production and grazing in a high-Arctic coastal marine ecosystem, Young Sound, Northeast Greenland. *Mar. Ecol. Prog. Ser.* **179**, 13–25 (1999).
24. Tamelander, T., Reigstad, M., Hop, H. & Ratkova, T. Ice algal assemblages and vertical export of organic matter from sea ice in the Barents Sea and Nansen Basin (Arctic Ocean). *Polar Biol.* **32**, 1261 (2009).
25. Watanabe, E. et al. Wind-driven interannual variability of sea ice algal production in the western Arctic Chukchi Borderland. *Biogeosciences* **12**, 6147–6168 (2015).
26. Limoges, A. et al. Spring succession and vertical export of diatoms and IP25 in a seasonally ice-covered high Arctic fjord. *Front. Earth Sci.* **6**, 226 (2018).
27. Lalande, C., Nöthig, E.-M. & Fortier, L. Algal export in the Arctic Ocean in times of global warming. *Geophys. Res. Lett.* **46**, 5959–5967 (2019).
28. Luostarinen, T. et al. An annual cycle of diatom succession in two contrasting Greenlandic fjords: from simple sea-ice indicators to varied seasonal strategies. *Mar. Micropaleontol.* **158**, 101873 (2020).
29. Head, M. J., Harland, R. & Matthiessen, J. Cold marine indicators of the late Quaternary: the new dinoflagellate cyst genus *Islandinium* and related morphotypes. *J. Quater. Sci.* **16**, 621–636 (2001).
30. de Vernal, A. et al. Reconstructing past sea ice cover of the Northern Hemisphere from dinocyst assemblages: status of the approach. *Quater. Sci. Rev.* **79**, 122–134 (2013).
31. Krawczyk, D. W. et al. Quantitative reconstruction of Holocene sea ice and sea surface temperature off West Greenland from the first regional diatom data set. *Paleoceanogr. Paleoclimatol.* **32**, 18–40 (2017).
32. Oksman, M., Juggins, S., Miettinen, A., Witkowski, A. & Weckström, K. The biogeography and ecology of common diatom species in the northern North Atlantic, and their implications for paleoceanographic reconstructions. *Mar. Micropaleontol.* **148**, 1–28 (2019).
33. Weckström, K. et al. Improving the paleoceanographic proxy tool kit – On the biogeography and ecology of the sea ice-associated species *Fragilariopsis oceanica*, *Fragilariopsis reginae-jahniae* and *Fossula arctica* in the northern North Atlantic. *Mar. Micropaleontol.* **157**, 101860 (2020).
34. Belt, S. T. et al. A novel chemical fossil of palaeo sea ice: IP25. *Org. Geochemist.* **38**, 16–27 (2007).
35. Brown, T. A., Belt, S. T., Tatarek, A. & Mundy, C. J. Source identification of the Arctic sea ice proxy IP25. *Nat. Commun.* **5**, 4197 (2014).
36. Belt, S. T. et al. Source identification and distribution reveals the potential of the geochemical Antarctic sea ice proxy IPSO25. *Nat. Commun.* **7**, 12655 (2016).
37. Belt, S. T. et al. Identification of paleo Arctic winter sea ice limits and the marginal ice zone: Optimised biomarker-based reconstructions of late Quaternary Arctic sea ice. *Earth Planetary Sci. Lett.* **431**, 127–139 (2015).
38. Smik, L., Cabedo-Sanz, P. & Belt, S. T. Semi-quantitative estimates of paleo Arctic sea ice concentration based on source-specific highly branched isoprenoid alkenes: A further development of the PIP25 index. *Org. Geochemist.* **92**, 63–69 (2016).
39. Rontani, J.-F., Belt, S. T., Vaultier, F., Brown, T. A. & Massé, G. Autoxidative and Photooxidative Reactivity of Highly Branched Isoprenoid (HBI) Alkenes. *Lipids* **49**, 481–494 (2014).
40. Ingram, R. G. & Prinsenberg, S. Coastal oceanography of Hudson Bay and surrounding eastern Canadian Arctic waters, coastal segments. In: *The Sea, vol. 11—The global coastal ocean, regional studies and syntheses* (Eds. Robinson, A.R. & Brink, K.H.) 835–861 (Chichester UK Wiley, 1998).
41. Macdonald, R. W. & Kuzyk, Z. A. The Hudson Bay system: A northern inland sea in transition. *J. Mar. Syst.* **88**, 337–340 (2011).
42. Déry, S. J., Mlynowski, T. J., Hernández-Henríquez, M. A. & Straneo, F. Interannual variability and interdecadal trends in Hudson Bay streamflow. *J. Mar. Syst.* **88**, 341–351 (2011).
43. Prinsenberg, S. J. The circulation pattern and current structure of Hudson Bay. In: *Canadian Inland Seas* (Ed. Martini, I.P.) 187–203 (Elsevier, 1986).
44. Granskog, M. A., Kuzyk, Z. Z., Azetsu-Scott, K. & Macdonald, R. W. Distributions of runoff, sea-ice melt and brine using  $\delta^{18}\text{O}$  and salinity data—A new view on freshwater cycling in Hudson Bay. *J. Mar. Syst.* **88**, 362–374 (2011).
45. Eastwood, R. A. et al. Role of river runoff and sea ice brine rejection in controlling stratification throughout winter in Southeast Hudson Bay. *Estuaries Coasts* **43**, 756–786 (2020).
46. Galbraith, P. S. & Larouche, P. Sea-surface temperature in Hudson Bay and Hudson Strait in relation to air temperature and ice cover break up, 1985–2009. *J. Mar. Syst.* **87**, 66–78 (2011).
47. Campbell, K., Mundy, C. J., Barber, D. G. & Gosselin, M. Characterizing the sea ice algae chlorophyll a–snow depth relationship over Arctic spring melt using transmitted irradiance. *J. Mar. Syst.* **147**, 76–84 (2015).
48. Lange, B. A. et al. Contrasting Ice Algae and Snow-Dependent Irradiance Relationships Between First-Year and Multiyear Sea Ice. *Geophys. Res. Lett.* **46**, 10834–10843 (2019).
49. Rau, G. H., Takahashi, T. & Marais, D. J. D. Latitudinal variations in plankton  $\delta^{13}\text{C}$ : implications for CO<sub>2</sub> and productivity in past oceans. *Nature* **341**, 516–518 (1989).
50. Pineault, S., Tremblay, J.-É., Gosselin, M., Thomas, H. & Shadwick, E. The isotopic signature of particulate organic C and N in bottom ice: Key influencing factors and applications for tracing the fate of ice-algae in the Arctic Ocean. *J. Geophys. Res. Ocean* **118**, 287–300 (2013).
51. de la Vega, C., Jeffreys, R. M., Tuerena, R., Ganeshram, R. & Mahaffey, C. Temporal and spatial trends in marine carbon isotopes in the Arctic Ocean and implications for food web studies. *Global Change Biol.* **25**, 4116–4130 (2019).
52. Kuzyk, Z. Z. A., Macdonald, R. W., Tremblay, J.-É. & Stern, G. A. Elemental and stable isotopic constraints on river influence and patterns of nitrogen cycling and biological productivity in Hudson Bay. *Continental Shelf Res.* **30**, 163–176 (2010).
53. Massé, G. et al. Abrupt climate changes for Iceland during the last millennium: Evidence from high resolution sea ice reconstructions. *Earth Planetary Sci. Lett.* **269**, 565–569 (2008).
54. Müller, J. et al. Holocene cooling culminates in sea ice oscillations in Fram Strait. *Quat. Sci. Rev.* **47**, 1–14 (2012).
55. Weckström, K. et al. Evaluation of the sea ice proxy IP25 against observational and diatom proxy data in the SW Labrador Sea. *Quater. Sci. Rev.* **79**, 53–62 (2013).
56. Hörner, T., Stein, R., Fahl, K. & Birgel, D. Post-glacial variability of sea ice cover, river run-off and biological production in the western Laptev Sea (Arctic Ocean)—A high-resolution biomarker study. *Quater. Sci. Rev.* **143**, 133–149 (2016).
57. Limoges, A. et al. Learning from the past: Impact of the Arctic Oscillation on sea ice and marine productivity off northwest Greenland over the last 9,000 years. *Global Change Biol.* **26**, 6767–6786 (2020).
58. Pienkowski, A. J. et al. Seasonal sea ice persisted through the Holocene Thermal Maximum at 80°N. *Commun. Earth Environ.* **2**, 124 (2021).
59. Belt, S. T., Smik, L., Köseoglu, D., Knies, J. & Husum, K. A novel biomarker-based proxy for the spring phytoplankton bloom in Arctic and sub-arctic settings – HBI T25. *Earth Planetary Sci. Lett.* **523**, 115703 (2019).
60. Collins, L. G. et al. Evaluating highly branched isoprenoid (HBI) biomarkers as a novel Antarctic sea-ice proxy in deep ocean glacial age sediments. *Quat. Sci. Rev.* **79**, 87–98 (2013).



61. Köseoğlu, D., Belt, S. T., Husum, K. & Knies, J. An assessment of biomarker-based multivariate classification methods versus the PIP25 index for paleo Arctic sea ice reconstruction. *Organic Geochemistry* **125**, 82–94 (2018).
62. Ringrose, A. E. Temporal and vertical distributions of IP25 and other lipid biomarkers in sea ice from Resolute Bay, Nunavut, Canada. MSc thesis, University of Plymouth. <http://hdl.handle.net/10026.1/2880> (2013).
63. Leu, E. et al. Spatial and Temporal Variability of Ice Algal Trophic Markers—With Recommendations about Their Application. *J. Mar. Sci. Eng.* **8**, 676 (2020).
64. Amiraux, R. et al. Temporal evolution of IP25 and other highly branched isoprenoid lipids in sea ice and the underlying water column during an Arctic melting season. *Element. Sci. Anthropocene* **7**, 38 (2019).
65. Mikkelsen, D. M., Rysgaard, S. & Glud, R. N. Microalgal composition and primary production in Arctic sea ice: a seasonal study from Kobbefjord (Kangerluarsunnguaq), West Greenland. *Mar. Ecol. Progr. Series* **368**, 65–74 (2008).
66. Brown, T. A. et al. Influence of nutrient availability on Arctic sea ice diatom HBI lipid synthesis. *Org. Geochem.* **141**, 103977 (2020).
67. Müller, J. et al. Towards quantitative sea ice reconstructions in the northern North Atlantic: A combined biomarker and numerical modelling approach. *Earth Planet. Sci. Lett.* **306**, 137–148 (2011).
68. Knies, J. et al. The emergence of modern sea ice cover in the Arctic Ocean. *Nat. Commun.* **5**, 5608 (2014).
69. Heikkilä, M. et al. Surface sediment dinoflagellate cysts from the Hudson Bay system and their relation to freshwater and nutrient cycling. *Mar. Micropaleontol.* **106**, 79–109 (2014).
70. Medlin, L. K. & Hasle, G. R. Some *Nitzschia* and related species from fast ice samples in the Arctic and the Antarctic. *Polar Biol.* **10**, 451–479 (1990).
71. von Quillfeldt, C. H., Ambrose, W. G. Jr. & Clough, L. M. High number of diatom species in first-year ice from the Chukchi Sea. *Polar Biol.* **26**, 806–818 (2003).
72. Ratkova, T. N. & Wassmann, P. Sea ice algae in the White and Barents Seas: composition and origin. *Polar Res.* **24**, 95–110 (2005).
73. Różanska, M., Gosselin, M., Poulin, M., Wiktor, J. M. & Michel, C. Influence of environmental factors on the development of bottom ice protist communities during the winter–spring transition. *Mar. Ecol. Prog. Ser.* **386**, 43–59 (2009).
74. Leu, E. et al. Arctic spring awakening: Steering principles behind the phenology of vernal ice algal blooms. *Prog. Oceanogr.* **139**, 151–170 (2015).
75. Dunbar, M. J. & Acreman, J. C. Standing crops and species composition of diatoms in sea ice From Robeson Channel to the Gulf of St. Lawrence. *Ophelia* **19**, 61–72 (1980).
76. Hop, H. et al. Changes in sea-ice protist diversity with declining sea ice in the Arctic Ocean from the 1980s to 2010s. *Front. Mar. Sci.* **7**, 243 (2020).
77. Campbell, K. et al. Melt procedure affects the photosynthetic response of sea ice algae. *Front. Earth Sci.* **7**, 21 (2019).
78. Brodie et al. Evidence for bias in C and N concentrations and  $\delta^{13}C$  composition of terrestrial and aquatic organic materials due to pre-analysis acid preparation methods. *Chem. Geol.* **282**, 67–83 (2011).
79. Battarbee, R. W. et al. Diatoms. In: *Tracking Environmental Change Using Lake Sediments Volume 3, Terrestrial, Algal, and Siliceous Indicators* (Eds. Smol, J.P., Birks, H.J.B., Last, W.M.) 155–202 (Kluwer Academic Publishers, 2001).
80. Stockmarr, J. Tablets with spores used in absolute pollen analysis. *Pollen Spores* **13**, 615–621 (1972).
81. Mertens, K. N. et al. Determining the absolute abundance of dinoflagellate cysts in recent marine sediments: The Lycopodium marker-grain method put to the test. *Rev. Paleobotany Palynol.* **157**, 238–252 (2009).
82. Mertens, K., Price, A. & Pospelova, V. Determining the absolute abundance of dinoflagellate cysts in recent marine sediments II: Further tests of the Lycopodium marker-grain method. *Rev. Paleobotany Palynol.* **184**, 74–81 (2012).
83. Poulin, M. & Cardinal, A. Sea ice diatoms from Manitounuk Sound, southeastern Hudson Bay (Quebec, Canada). I. Family Naviculaceae. *Can. J. Bot.* **60**, 1263–1278 (1982).
84. Poulin, M. & Cardinal, A. Sea ice diatoms from Manitounuk Sound, southeastern Hudson Bay (Quebec, Canada). II. Family Naviculaceae, genus *Navicula*. *Can. J. Bot.* **60**, 2825–2845 (1982).
85. Poulin, M. & Cardinal, A. Sea ice diatoms from Manitounuk Sound, southeastern Hudson Bay (Quebec, Canada). III. Cymbellaceae, Entonmoidaceae, Gomphonemataceae, Nitzschiaceae. *Can. J. Bot.* **61**, 107–118 (1983).
86. Cremer, H. The diatom flora of the Laptev Sea (Arctic Ocean). *Bibliotheca Diatomol.* **40**, 169 (1998). pp.
87. Witkowski, A., Lange-Bertalot, H. & Metzeltin, D. Diatom flora of marine coast I. In: *Inconographia Diatomologica. Annotated Diatom Micrographs vol. 7. Diversity-Taxonomy-Identification* (Ed. Lange-Bertalot, H.) 925 pp. (Koeltz Scientific Books, 2000).
88. Radi, T. et al. Operational taxonomy and (paleo-)autecology of round, brown, spiny dinoflagellate cysts from the Quaternary of high northern latitudes. *Mar. Micropaleontol.* **98**, 41–57 (2013).
89. Zonneveld, K. A. & Pospelova, V. A determination key for modern dinoflagellate cysts. *Palynology* **39**, 387–409 (2015).
90. Belt, S. T. et al. A reproducible method for the extraction, identification and quantification of the Arctic sea ice proxy IP25 from marine sediments. *Analyt. Methods* **4**, 705–713 (2012).
91. Chen, N., Bianchi, T. S., McKee, B. A. & Bland, J. M. Historical trends of hypoxia on the Louisiana shelf: applications of pigments as biomarkers. *Org. Geochem.* **32**, 543–561 (2001).
92. McGowan, S. Palaeolimnology: pigment studies. In: *Encyclopedia of Quaternary Science. 2nd edition* (Eds. Elias S.A., Mock C.J.) 326–338 (Elsevier, 2013).
93. Leavitt, P. R. & Hodgson D. A. Sedimentary pigments. In: *Tracking Environmental Change using Lake Sediments. Volume 3: Terrestrial, Algal, and Siliceous Indicators* (Eds. Smol J.P., Birks, H.J.B., Last, W.M.) 295–325 (Kluwer Academic Publishers, 2013).

## Acknowledgements

This study was funded by the Academy of Finland (grants 1296895, 1307282 and 1328540), The Alfred Kordelin Foundation, ArcticNet Networks of Centres of Excellence (NCE), Natural Sciences and Engineering Research Council of Canada (NSERC) Discovery Grant Programs, Polar Knowledge Canada and Arctic Avenue. Open access was funded by Helsinki University Library. We thank Joel Heath, Johnny Kudluarok, Puasi Ippak, Johnassie Inuktaluk, Johnny Ippak, Ronnie Ippak, Charlie Novalinga, Lucy Ann Novalinga, Lucassie Arragutainaq, Arctic Eider Society, Sanikiluaq Hunters and Trappers Association, Meeri Näppilä, Heini Ali-Kovero, Caroline Guilmette, Alessia Guzzi, Emmelia Stainton and Linda Chow for their valuable help. We also kindly acknowledge the helpful comments of two anonymous reviewers.

## Author contributions

M.H. supervised and conceptualised the project. M.H., Z.Z.K., J.E. and M.K. designed the field campaign, and Z.Z.K., J.E., M.K., T.L. and A.D. conducted the fieldwork. T.L. carried out all sample preparations and data treatment. T.L. carried out the microscopic identifications and counts for diatoms (water column, sediment trap, surface sediment), K.W. for diatoms (sea ice) and M.H. for dinoflagellate cysts. A.B. and S.M. oversaw the pigment analyses and G.M. the biomarker analyses. J.E. designed the mooring line setup and interpreted the CTD data. T.L., M.H. and K.W. interpreted the data and wrote the paper. All authors discussed the results and implications, commented and contributed to the paper. T.L. is the corresponding author.

## Competing interests

The authors declare no competing interests.

## Additional information

**Supplementary information** The online version contains supplementary material available at <https://doi.org/10.1038/s43247-023-00719-3>.

**Correspondence** and requests for materials should be addressed to Tiia Luostarinen.

**Peer review information** *Communications Earth & Environment* thanks the anonymous reviewers for their contribution to the peer review of this work. Primary Handling Editor: Joe Aslin. Peer reviewer reports are available.

**Reprints and permission information** is available at <http://www.nature.com/reprints>

**Publisher's note** Springer Nature remains neutral with regard to jurisdictional claims in published maps and institutional affiliations.



**Open Access** This article is licensed under a Creative Commons

Attribution 4.0 International License, which permits use, sharing, adaptation, distribution and reproduction in any medium or format, as long as you give appropriate credit to the original author(s) and the source, provide a link to the Creative Commons license, and indicate if changes were made. The images or other third party material in this article are included in the article's Creative Commons license, unless indicated otherwise in a credit line to the material. If material is not included in the article's Creative Commons license and your intended use is not permitted by statutory regulation or exceeds the permitted use, you will need to obtain permission directly from the copyright holder. To view a copy of this license, visit <http://creativecommons.org/licenses/by/4.0/>.

© The Author(s) 2023